Synthesis, biological activities of chalcones and novel 4-acetylpyridine oximes, molecular docking of the synthesized products as acetylcholinesterase ligands

Kamilia Ould Lamara, Malika Makhloufi-Chebli, Amina Benazzouz-Touami, Souhila Terrachet-Bouaziz, Anthony Robert, Carine Machado-Rodrigues, Jean-Bernard Behr

ELSEVIER

Journal of Molecular Structure
journal homepage: www.elsevier.com

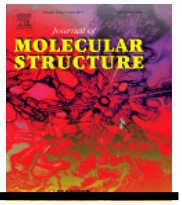

Synthesis, Biological activities of chalcones and novel 4-acetylpyridine oximes, molecular docking of the synthesized products as acetylcholinesterase ligands

Kamilia Ould Lamara,[a] Makhloufi-Chebli Malika,[a] Amina Benazzouz-touami,[a] Souhila Terrachet-Bouaziz,[b,c] Anthony Robert,[d] Carine Machado-Rodrigues,[d] Jean-Bernard Behr [d**]*

[a]*Laboratoire LPCM, Département de Chimie, Faculté des Sciences, Université Mouloud Mammeri, 15000, Tizi-Ouzou, Algeria.*

[b] *Department of Chemistry, Faculty of Sciences, University Mohamed Bouguerra, Boumerdes, Algeria.*

[c] *Laboratoire de Physico-Chimie Théorique et de Chimie Informatique, Faculté de Chimie, USTHB, BP 32 El Alia, 16111 Bab-Ezzouar, Alger, Algeria.*

[d]*Université de Reims Champagne –Ardenne, Institut de Chimie Moléculaire de Reims (ICMR), CNRS UMR 7312, UFR Sciences Exactes et Naturelles, BP 1039, 51687 Reims Cedex 2, France.*

ARTICLE INFO

Article history:
Received
Received in revised form
Accepted
Aqavailable online

Keywords:
heterocyclic chalcones
oximes
antioxidant capacity
antimicrobial activity
Molecular docking
acetylcholinesterase inhibitors
fep-mAChE protein

ABSTRACT

Heterocyclic chalcones were synthesized by the reaction of 4-acetylpyridine with the corresponding aromatic aldehyde under *Claisen Schmidt* conditions. These chalcones were used as starting material for the synthesis of oximes in the presence of hydroxylamine hydrochloride. The structures of the synthesized compounds were confirmed by IR, ^{1}H NMR, ^{13}C NMR and ESI-MS, HRMS spectral analyses. All the synthesized compounds were evaluated for their antioxidant activity by DPPH• method and their *in vitro* antimicrobial activity by disk diffusion method against two Gram-negative bacteria, one Gram-positive bacteria and two fungal strains (*C. albicans* and *A. niger)*. The results showed that the synthesized compounds did not display significant antioxidant activity. However, compounds **3b**, **3d**, **3f**, **3h**, **3i** showed excellent antibacterial activity better than the standard drug against the bacterial strain *S. aureus* (ATCC 25923). The two compounds **3c**, **3d** proved very active against the fungal strain *A. niger* (**MIC= 7.81 µg/ mL**, **15.62 µg/mL** respectively) while the antifungal drug used as reference (Fluconazole) was inactive. Molecular docking and molecular dynamics results revealed that the synthesized compounds, **4e**, **4c**, and **5j**, were involved in a large number of favorable interactions with the active site residues of the acetylcholinesterase protein, which can stabilize the ligands in the active site and increase their affinities.

1. Introduction [1]

The damage caused by bacterial and fungal infections has deeply increased in recent years [1]. Infectious diseases caused by bacterial pathogens have become a major public health issue due to the emergence of drug resistance, which resulted in increased mortality and morbidity due to treatment failure [2, 3]. Several bacterial strains that seemed to be under control are again causing deaths each year due to the lack of appropriate antibiotic drugs [4]. Particular attention has focused on the Gram-positive organism *Staphylococcus aureus* because many strains are now resistant to standard antibiotics such as methicillin and vancomycin [5]. The occurrence of multi-drug resistant bacteria becomes a severe medical setback in hospital and community settings [2]. Among them, methicillin-resistant *Staphylococcus aureus* (MRSA), penicillin resistant *Streptococcus pneumoniae* (PRSP), and vancomycin resistant *Enterococci* (VRE) are leading concerns [6, 7]. Even though the MRSA occurs naturally in the human flora of skin and especially nasal mucosa, it is an opportunistic pathogen frequently found in nosocomial infections that may lead to severe infections, including septicemias [8]. Therefore, the synthesis of new lead structures and chemical entities for the development of antimicrobial agents with unprecedented mode of actions is an important task in medical field.

Chalcones are a plethora of natural and synthetic compounds, which present a reactive α,β-

[1]Corresponding authors.
E-mail adresses : makhloufi_malika@yahoo.fr (MM),
jb.behr@univ-reims.fr (JBB)

unsaturated carbonyl system into their structures. This particularity generates a wide spectrum of biological activities including anti-inflammatory [9, 10], antioxidant [11,12], antitumor [13-15], antidiabetic [16], or antimicrobial [17]. As electrophilic scaffolds, chalcones are easily converted into more elaborated therapeutically important heterocyclic molecules [12, 18]. Natural or synthetic analogues of chalcone, such as oxime-like derivatives, have been reported to exhibit various antimicrobial [19,20], antifungal [20] and tyrosinase inhibitory activities, respectively [21,22]. As previously reported, many compounds with oxime groups display potent biological activities and low toxicities [22, 23]. Some of them have been used as clinical medical agents and some have been reported as acetylcholinesterase inhibitors [24].

Based on our previous work [25], we investigated further the potential of biological active molecules of natural origin. Therefore, in this work, we describe the synthesis of a series of chalcones from 4-acetylpyridine and a new series of chalcone-oximes and their evaluation as antimicrobial agents against a series of bacterial and fungal strains, in view of existing activities for analogous structures. Most of the chalcones are known compounds [26], however, their biological activity was not evaluated yet. Furthermore, all of the oximes are unknown. In addition, the synthesized compounds were evaluated for their antioxidant activity by the DPPH$^{\bullet}$ method. Finally, since oximes are known to counteract the negative effects of nerve agents by means of their potent affinity for acetylcholinesterase, molecular docking and molecular dynamics experiments were conducted with new oximes **4** to assess their affinities with an acetylcholinesterase and predict their potential to restore the enzymatic activity.

2. Experimental

2.1. Materials and methods

All reagents were purchased from Aldrich. They were of analytical grade and were used without further purification. Melting points were determined on a Stuart scientific SPM3 apparatus fitted with a microscope and are uncorrected. ^{1}H and ^{13}C NMR spectra were recorded in DMSO-d_6 or in $CDCl_3$ solutions on Bruker Avance 300 (300.13 *MHz* for ^{1}H and 75.47 *MHz* for ^{13}C) or on Bruker Avance Neo 500 (500.28 *MHz* for ^{1}H, 125.8 *MHz* for ^{13}C) spectrometer. Chemical shifts are expressed in parts per million (δ, ppm). They were recorded relative to solvent signal or TMS signal. The coupling constants (*J*) are given in hertz (Hz) and splitting pattern abbreviations are: s, singlet; app s, apparent singlet; d, doublet; t, triplet; m, multiplet. Mass spectra are obtained with ESI. Positive-ion ESI mass spectra were acquired using a Q-TOF 2 instrument, sample solution (10^{-5} M) in 200 µL of 0.1% trifluoroacetic acid/methanol. Nitrogen was used as nebulizer gas and argon as collision gas. The needle voltage was set at 3000 V, with the ion source at 80 °C and desolvation temperature at 150 °C. Cone voltage was 35 V. Samples were alternatively analyzed by ESI/Q-TOF HRMS method. The MS analysis was performed on a Waters SYNAPT G2-Si High Resolution Mass Spectrometry equipped with electrospray ionization source ESI (Waters Corp., Manchester, UK). Mass detection was conducted in positive ion mode, with the source temperature at 100◦C, capillary voltage and cone voltage were set at 3 kV and 40 V. The desolvation gas was optimized to 600 L/h, the cone gas flow at 50 L/h and the scan range was from 50 to 1600 m/z. Analysis were realized in infusion mode, mass was corrected during acquisition using external reference (Lock-Spray) of 1 ng/uL solution of leucine encephalin at a flow rate of 10 µL/min. All data collected were acquired using MassLynxTM (V4.1) software in centroid mode.

2.2. *General procedure for the synthesis of compounds (3a-j)*

Method A [26]: To a cooled solution of 10 % NaOH, 1.0 equiv of liquid aldehydes was added. To this solution 1.0 equiv of 4-acetyl pyridine was added dropwise over a 30 min period. The solution was maintained at 0°C for an hour and then was allowed to stir at rt. After some time a solid separated out. The solution was further stirred for about 1h. The solid was filtered off and then recrystallized from methanol or ethanol to give crystals of the chalcone.

Method B [26]: In the case of aldehydes in a solid state, the aldehyde (1 equiv) was first dissolved in minimum quantity of ethanol or methanol (approx 10 mL) and then 10 % NaOH solution (approx 100 mL) was added to give a clear solution. The solution was cooled up to 0°C by applying ice bath below it. Then 1 equiv of 4-acetyl pyridine was added dropwise over 30 min. The solution was maintained at 0°C for 1h and then was allowed to stir at room temperature. After some time a solid started separating out. This was stirred for about an hour. The solid was filtered off and then recrystallized from methanol or ethanol to give crystals of the chalcones.

Method C [27]: Indole-3-carboxaldehyde (1 equiv) was reacted with 4-acetyl-pyridine (1 equiv) in presence of piperidine (0.5 equiv) using methanol as solvent. The reaction mixture was stirred under reflux for 16 hours. After the completion of the reaction, yellow-orange colored precipitate was filtered, washed, dried and recrystallized from ethanol-dichloromethane to furnish precursor **(3j)**.

2.2.1. (E)-1-(pyridin-4-yl)-3-(thiophen-2-yl)prop-2-en-1-one (3a)

Compound **3a** was obtained from 4-acetylpyridine and thiophene-2-carbaldehyde, using procedure A.

Pistachio crystalline powder; Yield: 62 % ; m.p: 103-105 °C (lit.[28] mp : 98-100 °C) ; FT-IR (cm^{-1}): 3075 (aromatic C-H), 1662 (C=O), 1579 (aromatic C=C), 1413 (C=N), 965 (-CH=CH- trans),

709 (C-S) ; UV/Vis : λabs ($CHCl_3$)/nm 355- 242 ; ^{1}H NMR (300 MHz, DMSO-d_6) : δ 7.23 (dd, *J=3.7Hz*, *J=5.0Hz*, 1H, ArH-thio), 7.51 (d, *J= 15.4 Hz*, 1H, =CH), 7.76 (m , 1H, ArH-thio), 7.86 (m , 1H, ArH-thio), 7.94 (m, 2H, ArH-py), 7.98 (m, 1H, =CH), 8.84 (m, 2H, ArH-py) ; ^{13}C NMR (75MHz, DMSO-d_6): δ 119.84, 121.50, 128.88, 131.44, 133.76, 138.38, 139.41, 143.58, 150.74, 188.72 ; MS (ESI+) : m/z = 216,10 $[M+H]^+$ (100%).

2.2.2. (E)-1-(pyridin-4-yl)-3-(thiophen-3-yl)prop-2-en-1-one (3b)

Compound **3b** was obtained from 4-acetylpyridine and thiophene-3-carbaldehyde, using procedure A.

Brown crystalline powder ; Yield: 70 %; m.p: 110-112 °C; FT-IR (cm^{-1}) : 3095 (aromatic C-H), 1662 (C=O), 1585 (aromatic C=C), 1543 (C=N), 987 (-CH=CH-trans), 781 (C-S); UV/Vis: λabs: ($CHCl_3$)/nm 329-240 ; ^{1}H NMR (300 MHz, DMSO-d_6): δ 7.70 (m, 1H, ArH-thio), 7.71 (d, *J=15.4 Hz*, 1H, =CH), 7.79 (m, 1H, ArH-thio) 7.83 (d, *J=15.4 Hz*, 1H, =CH), 7.97 (m, 2H, ArH-py), 8.19 (m, 1H, ArH-thio), 8.85 (m, 2H, ArH-py) ;^{13}C NMR (75 MHz, DMSO-d6): δ 120.92, 121.44, 125.16, 127.38, 130.36, 137.70, 140.00, 144.39, 150.75, 189.99; MS (ESI+): m/z = 216,10 $[M+H]^+$ (100%).

2.2.3. (2E,4E)-1-phenyl-5-(pyridin-4-yl)penta-2,4-dien-1-one (3c)

Compound **3c** was obtained from 4-acetylpyridine and 3-phenylacrylaldehyde, using procedure A.

Green crystalline powder; Yield: 72 % ; m.p: 95-98 °C ; FT-IR (cm^{-1}) 3046 (aromatic C-H), 1651 (C=O), 1576 (aromatic C=C), 1417 (C=N), 1007 (-CH=CH- trans), 699 (C-H bending vibration of deformation of benzene ring 5 adjacent hydrogens atoms); UV/Vis : λabs ($CHCl_3$)/nm 354-242 ; ^{1}H NMR (300 MHz, DMSO-d_6): δ 7.26-7.35 (3H, (1H, =CH) (2H, Ar-H)), 7.37- 7.48 (m, 3H, (2H, =CH), (1H Ar-H)), 7.54- 7.66 (m, 3H, (1H, =CH) (2H Ar-H)), 7.85 (m, 2H, ArH-py), 8.84 (m, 2H, ArH-py) ; ^{13}C NMR (75 MHz, DMSO-d_6): δ 121.35, 124.98, 127.03, 127.44, 128.98, 129.51, 135.84 , 143.04, 143.77, 146.20, 150.77, 189.29; MS (ESI+): m/z = 236,20 $[M+H]^+$ (100%).

2.2.4. (E)-3-phenyl-1-(pyridin-4-yl)prop-2-en-1-one (3d)

Compound **3d** was obtained from 4-acetylpyridine and benzaldehyde, using procedure A.

Fine yellowish powder; Yield: 75 %; m.p: 175-177 °C (lit.[26] mp : 172-174 °C) ; FT-IR (cm^{-1}): 3055 (aromatic C-H), 1663 (C=O), 1595 (aromatic C=C), 1446 (C=N), 984 (-CH=CH- trans), 686 (C-H bending vibration of deformation of benzene ring 5 adjacent hydrogens atoms); UV/Vis: λabs ($CHCl_3$)/nm 316-242; ^{1}H NMR (500 MHz, $CDCl_3$): δ 7.42 (d, *J=15.8Hz*, 1H, =CH), 7.41-7.48 (m, 3H, ArH), 7.62-7.68 (m, 2H, Ar-H), 7.79 (m, 2H, ArH-py), 7.83 (d, *J= 15.8 Hz*, 1H, =CH), 8.84 (m, 2H, ArH-py) ; ^{13}C NMR (125 MHz, $CDCl_3$): δ 121.27, 121.80, 128.86, 129.25, 131.40, 134.40, 144.84, 147.14, 150.60, 189.87; HRMS (ESI+): m/z = 210,0920 $[M+H]^+$ (100%).

2.2.5. (E)-3-(4-methoxyphenyl)-1-(pyridin-4-yl)prop-2-en-1-one (3e)

Compound **3e** was obtained from 4-acetylpyridine and 4-methoxybenzaldehyde, using procedure B.

Yellow crystalline powder ; Yield: 75 %; m.p: 115-117 °C (lit.[26] mp : 104-106 °C) ; FT-IR (cm^{-1}) : 3060 (aromatic C-H), 1658 (C=O), 1588 (aromatic C=C), 1508 (C=N), 987 (-CH=CH- trans), 813 (C-H bending vibration of p-disubstituted benzene ring ($-OCH_3$)) ; UV/Vis : λabs($CHCl_3$)/nm 352-242; ^{1}H NMR (300 MHz, DMSO-d_6): δ 3.84 (s, 3H, OCH_3), 7.04 (m, 2H, Ar-H), 7.77 (m, 2H, =CH), 7.89 (m, 2H, Ar-H), 7.99 (m, 2H, ArH-py), 8.84 (m, 2H, ArH-py) ; ^{13}C NMR (75 MHz, DMSO-d_6): δ 55.44, 114.50, 119.03, 121.56, 127.00, 131.20, 143.90, 145.77, 150.72, 161.79, 188.92; MS (ESI+): m/z = 240,20 $[M+H]^+$ (100%).

2.2.6. (E)-3-(4-nitrophenyl)-1-(pyridin-4-yl)prop-2-en-1-one (3f)

Compound **3f** was obtained from 4-acetylpyridine and 4-nitrobenzaldehyde, using procedure B.

Fine grey powder ; Yield: 83 %; m.p: 170-172 °C (lit.[29] mp: 187-189 °C); FT-IR (cm^{-1}) : 3130 (aromatic C-H), 1698 (C=O), 1581 (aromatic C=C), 1508 (C=N), 1000 (-CH=CH- trans), 1348 (C-NO_2) , 816 (C-H bending vibration of p-disubstituted benzene ring) ; UV/Vis : λabs ($CHCl_3$)/nm 284; ^{1}H NMR (300 MHz, DMSO-d_6): δ 5.82 (m, 1H, =CH), 7.71 (d, *J= 9.0 Hz*, 2H, ArH-NO_2), 7.83-7.86 (m, 2H, ArH-py), 8.19- 8.31 (m, *2H*, ArH-NO_2), 8.28 (m, 1H, =CH), 8.79- 8.81 (m, 2H, ArH-py); ^{13}C NMR (75 MHz, DMSO-d_6): δ 121.57, 123.75, 124.41, 127.68, 141.23, 143.17, 147.03, 151.24, 150.85, 192.04; MS (ESI+): m/z = 554.70 $[2M+ 2 Na]^+$ (100%).

2.2.7. (E)-3-(3-nitrophenyl)-1-(pyridin-4-yl)prop-2-en-1-one (3g)

Compound **3g** was obtained from 4-acetylpyridine and 3-nitrobenzaldehyde, using procedure B.

Fine off-white powder; Yield 73 %; m.p: 180-182 °C; FT-IR (cm^{-1}) : 3036 (aromatic C-H), 1667 (C=O), 1605 (aromatic C=C), 1520 (C=N), 995 (-CH=CH- trans), 1342 (C-NO_2) , 813 (C-H bending vibration of deformation of disubstituted benzene ring); UV/Vis : λabs ($CHCl_3$)/nm 296- 241; ^{1}H NMR (500 MHz, $CDCl_3$/drops of CH_3OD): δ 7.55 (d, *J=15.8Hz*, 1H, =CH), 7.63 (t, J=8.0Hz, 1H, ArH-NO_2), 7.85 (m, 2H, ArH-Py), 7.86 (m, 1H, =CH), 7.93 (d, *J=8.0 Hz*, 1H, ArH-NO_2) 8.28 (m, 1H, ArH- NO_2), 8.51 (m, 1H, ArH-NO_2), 8.86 (m, 2H, ArH-Py) ^{13}C NMR (125 MHz, $CDCl_3$/drops of CH_3OD): δ 121.94, 122.75, 123.57, 125.42, 130.36, 134.64, 136.06,

143.95, 144.34, 148.88, 150.45, 189.03 ; HRMS (ESI+) m/z calcd for $C_{14}H_{11}N_2O_3[M+H]^+$ 255.0770 found 255.0770.

2.2.8. (E)-3-(4-chlorophenyl)-1-(pyridin-4-yl)prop-2-en-1-one (3h)

Compound **3h** was obtained from 4-acetylpyridine and 4-chlorobenzaldehyde, using procedure B.

Light green crystalline powder; Yield: 72 %; m.p: 143-145 °C (lit.[30] mp : 139-141 °C) ; FT-IR (cm^{-1}): 3027 (aromatic C-H), 1671 (C=O), 1581 (aromatic C=C), 1486 (C=N), 978 (-CH=CH- trans), 811 (C-H bending vibration of p-disubstituted benzene ring (C-Cl)) ; UV/Vis : λabs ($CHCl_3$)/nm 320-242; ^{1}H NMR (300 MHz, DMSO-d_6): δ 7.56 (d, J=8.5Hz, 2H, ArH-Cl), 7.80 (d, J=15.7Hz, 1H, =CH), 7.94 (d, J=15.7Hz, 1H (1H, =CH)), 7.97 (d, J=8.5Hz, 2H, ArH-Cl) 8.01 (m, 2H, ArH-py), 8.86 (m, 2H, ArH-py); ^{13}C NMR (75MHz, DMSO-d_6): δ 122.08, 122.74, 129.49, 131.32, 133.80, 136.07, 143.89, 144.63, 151.26, 185.58; MS (ESI+): m/z = 244.1 $[M+H, {}^{35}Cl]^+$ (100%) , 246.10 $[M+H, Cl^{37}]^+$ (33.3%).

2.2.9. (E)-3-(2,6-dichlorophenyl)-1-(pyridin-4-yl)prop-2-en-1-one (3i)

Compound **3i** was obtained from 4-acetylpyridine and 2,6-dichlorobenzaldehyde, using procedure B.

Fine off-white powder; Yield: 70%; m.p: 100-102 °C; FT-IR (cm^{-1}) : 3087 (aromatic C-H), 1679 (C=O), 1575 (aromatic C=C), 1376 (C=N), 969 (-CH=CH- trans), 825 (C-H bending vibration of disubstituted benzene ring (C-Cl)) ; UV/Vis : λabs($CHCl_3$)/nm : 260; ^{1}H NMR (300 MHz, DMSO-d_6): δ 7.47 (dd, *J=7.4Hz, J=8.7Hz*, 1H, ArH-Cl), 7.62 (m, 2H, ArH-Cl), 7.77 (app s, 2H,=CH), 7.92 (m, 2H, ArH-py), 8.87 (m, 2H, ArH-py); ^{13}C NMR (75 MHz, DMSO-d_6): δ 121.55, 129.18, 129.95, 131.36, 131.66, 134.20, 138.43, 142.80, 150.96, 189.26; MS (ESI+): m/z = 278.1 $[M+H, {}^{35}Cl]^+$ (100%), 280.1 $[M+H, Cl^{37}]^+$ (63.9%).

2.2.10. (2E)-3-(1H-indol-3-yl)-1-(pyridin-4-yl)prop-2-en-1-on (3j)

Compound **3j** was obtained from 4-acetylpyridine and 1*H*-indole-2-carbaldehyde, using procedure C.

Fine orange-yellow powder; Yield: 90 %; m.p: 264-266 °C (lit.[27] mp : 266-268 °C); FT-IR (cm^{-1}): 3039 (N-H), 1648 (C=O), 1607 (C=C); UV/Vis : λabs (DMSO)/nm : 405; ^{1}H NMR (300 MHz, DMSO-d_6) δ (ppm): 7.22- 7.29 (m, 2H, Indol), 7.50-7.53 (m, 1H, Indol), 7.60 (d, 1H, *J=15.6 Hz*, =CH), 7.98 (m, 2H, ArH-py), 8.09-8.18 (m, 3H, (1H, =CH), (2H, Indol)), 8.83 (m, 2H, ArH-py), 12.02 (s, 1H, NH); ^{13}C NMR (75 MHz, DMSO-d_6) δ (ppm): 113.04, 113.35, 115.21, 121.02, 121.88, 121.94, 123.39, 125.55, 134.89, 138.12, 141.33, 145.23, 151.07, 188.89; MS (ESI+): m/z = 249.10 $[M+1]^+$.

2.3. General procedure for the synthesis of compounds 4

A mixture of substituted chalcones **3** (2 mmol), hydroxylamine hydrochloride (4 mmol) and anhydrous sodium acetate (4 mmol) in ethanol was refluxed for 2-5 h. After completion of the reaction, the mixture was cooled and poured into ice cold water. The resulting solid product **4** was filtered, washed with sufficient cold water, dried and purified by recrystallization from diluted ethanol (40%).

2.3.1. (1Z,2E)-1-(pyridin-4-yl)-3-(thiophen-2-yl)prop-2-en-1-one oxime (4a)

Compound **4a** was obtained from 1-(pyridin-4-yl)-3-(thiophen-2-yl)prop-2-en-1-one and hydroxylamine hydrochloride, using the procedure described above.

Yellow crystalline powder; mp: 210-212 °C; Yield : 42 % ; UV/Vis : λabs (DMSO)/nm : 324; ^{1}H NMR (500 MHz, DMSO-d_6): δ 7.11 (dd, *J=3.6Hz, J=5.0 Hz*, 1H, ArH-thio), 7.14-7.24 (m, 2H, =CH), 7.33 (m, 1H, ArH-thio), 7.65 (d, *J= 5.0 Hz*, 1H, ArH-thio, 8.04 (m, 2H, ArH-py), 8.91 (m, 2H, ArH-py), 12.68 (s, 1H, NOH); ^{13}C NMR (125 MHz, DMSO-d_6): δ 114.07, 125.72, 128.27, 128.46, 130.18, 131.15, 140.86, 143.41, 150.08, 151.92; HRMS (ESI+) m/z calcd for $C_{12}H_{11}N_2OS$ $[M+H]^+$ 231.0592 found 231.0592

2.3.2. (1Z,2E)-1-(pyridin-4-yl)-3-(thiophen-3-yl)prop-2-en-1-one oxime (4b)

Compound **4b** was obtained from 1-(pyridin-4-yl)-3-(thiophen-3-yl)prop-2-en-1-one and hydroxylamine hydrochloride, using the procedure described above.

Grey crystalline powder; mp: 203-205°C; Yield : 47 % ; UV/Vis : λabs (DMSO)/nm : 299; ^{1}H NMR (500 MHz, DMSO-d_6): δ 7.02 (d, *J=16.9 Hz*, 1H, =CH), 7.32 (d, *J= 16.9 Hz*, 1H, =CH), 7.54 (m, 1H, ArH-thio), 7.62 (m, 1H, ArH-thio), 7.76 (m, 1H, ArH-thio), 8.07 (m, 2H, ArH-py), 8.91 (m, 2H, ArH-py), 12.64 (s, 1H, NOH); ^{13}C NMR (125 MHz, DMSO-d_6): δ 115.15, 125.26, 125.66 , 127.20, 127.64, 132.45, 138.84, 143.16, 150.63, 152.23 ; HRMS (ESI+) m/z calcd for $C_{12}H_{11}N_2OS$ $[M+H]^+$ 231.0592 found 231.0594.

2.3.3. (1Z,2E,4E)-5-phenyl-1-(pyridin-4-yl)penta-2,4-dien-1-one oxime (4c)

Compound **4c** was obtained from 1-phenyl-5-(pyridin-4-yl)penta-2,4-dien-1-one and hydroxylamine hydrochloride, using the procedure described above.

Light yellow crystalline powder, mp: 233-235 °C; Yield: 40 % ; UV/Vis: λabs (DMSO)/nm :

329; ^{1}H NMR (500 MHz, DMSO-d_6): δ 6.84(d, *J=15.7Hz*, 1H, =CH), 6.82 (m, 1H, =CH), 7.07 (d, *J= 16.0 Hz*, 1H, =CH), 7.22 (dd, *J=10.7 Hz*, *J=15.5Hz*, 1H, =CH), 7.29 (m, 1H, ArH), 7.37 (m, 2H, ArH), 7.53 (m, 2H ArH), 8.05 (m, 2H, ArH-py), 8.93 (m, 2H, ArH-py), 12.68 (s, 1H, NOH); ^{13}C NMR (125 MHz, DMSO-d_6): δ 118.86, 125.73, 126.90, 128.57, 128.80, 136.30, 137.57, 138.86, 142.90, 150.80, 152.15 ; HRMS (ESI+) m/z calcd for $C_{16}H_{15}N_2O$ $[M+H]^+$ 251.1184 found 251.1186.

2.3.4. (1Z,2E)-3-(4-methoxyphenyl)-1-(pyridin-4-yl)prop-2-en-1-one oxime (4e)

Compound **4e** was obtained from 3-(4-methoxyphenyl)-1-(pyridin-4-yl)prop-2-en-1-one and hydroxylamine hydrochloride, using the procedure described above.

White crystalline powder, mp: 227-229 °C; Yield: 47 %; UV/Vis: λabs (DMSO)/nm : 319 ; ^{1}H NMR (500 MHz, DMSO-d_6): δ 3.78 (s, 3H, OCH_3), 6.93 (d, *J=17.0Hz*, 1H, =CH), 6.97 (m, 2H, ArH-OCH_3), 7.35 (d, *J=17.0 Hz*, 1H =CH), 7.57 (m, 2H, ArH-OCH_3), 8.08 (m, 2H, ArH-py), 8.92 (m, 2H, ArH-py), 12.60 (s, 1H, NOH); ^{13}C NMR (125 MHz, DMSO-d_6): δ 55.28, 113.18, 114.36, 125.79, 128.24, 129.04, 137.77, 142.90, 150.93, 152.34, 160.34; HRMS (ESI+) m/z calcd for $C_{15}H_{15}N_2O$ $[M+H]^+$ 255.1134 found 255.1133.

2.3.5. (1Z,2E)-3-(4-chlorophenyl)-1-(pyridin-4-yl)prop-2-en-1-one oxime (4h)

Compound **4h** was obtained from 3-(4-chlorophenyl)-1-(pyridin-4-yl)prop-2-en-1-one and hydroxylamine hydrochloride, using the procedure described above.

White powder; mp: 230-232 °C; Yield: 46% ; UV/Vis: λabs (DMSO)/nm : 301; ^{1}H NMR (500 MHz, DMSO-d_6): δ 7.02 (d, *J= 16.9 Hz*, 1H, =CH), 7.46 (m, 2H, ArH-Cl), 7.48 (d, *J=16.9 Hz*, 1H, =CH),7.66 (m, 2H, ArH-Cl) 8.12 (m, 2H, ArH-py), 8.94 (m, 2H, ArH-py) 12.85 (s, 1H, NOH); ^{13}C NMR (125 MHz, DMSO-d_6): δ 116.24, 125.78, 128.91, 129.17, 133.82, 134.68, 136.75, 142.63, 150.86, 151.80; HRMS (ESI+) m/z calcd for $C_{14}H_{12}N_2OCl$ $[M+H]^+$ 259.0638 found 259.0636.

2.3.6. (2E)-3-(2,6-dichlorophenyl)-1-(pyridin-4-yl)prop-2-en-1-one oxime (4i)

Compound **4i** was obtained from 3-(2,6-dichlorophenyl)-1-(pyridin-4-yl)prop-2-en-1-one and hydroxylamine hydrochloride, using the procedure described above.

Mixture of (*E*) and (*Z*) oximes, white powder; mp: 220-222 °C; Yield: 44 % ; UV/Vis : λabs (DMSO)/nm : 277; ^{1}H NMR (500 MHz, DMSO-d_6): δ 6.37 (d, J= 16.9Hz, 0.4H =CH^{oxim-b}), 6.96 (d, J=17.2Hz, 1H, =CH^{oxim-a}), 7.06 (d, J= 16.9 Hz, 0.4H =CH^{oxim-b}), 7.34 (m, 0.4H, Ar-H^{oxim-b}), 7.37 (d, J=17.3Hz, 1H, =CH^{oxim-a}), 7.40 (m, 1H, ArH^{oxim-a}),7.52 (m, 0.8H, Ar-H^{oxim-b}), 7.57 (m, 2H, Ar-H^{oxim-a}), 7.91(m, 0.8 H, ArH-py^{oxim-b}), 8.12 (m, 2H, ArH-py^{oxim-a}), 8.96 (m, 2H, ArH-py^{oxim-a}), 9.00 (m, 0.8 H, ArH-py^{oxim-b}), 12.26 (s, 0.4H, NOH^{oxim-b}), 13.00 (s, 1H, NOH^{oxim-a}); ^{13}C NMR (125 MHz, DMSO-d_6): δ 124.15, 125.29, 126.40, 128.86, 128.97, 129.01, 130.11, 130.51, 131.92, 132.59, 132.68, 132.92, 133.40, 133.55, 143.20, 144.14, 146.83, 149.83, 151.23, 152.80 ; HRMS (ESI+) m/z calcd for $C_{14}H_{11}N_2OCl_2$ $[M+H]^+$ 293.0248 found 293.0248.

2.4. General procedure for the synthesis of compound 5

A mixture of substituted chalcone **3j** (2 mmol), hydroxylamine hydrochloride (4 mmol) and anhydrous sodium acetate (4 mmol) in ethanol was refluxed for 13 h. After completion of the reaction, the reaction mixture was cooled. The resulting pale green solid product was filtered, washed with sufficient cold water, dried and purified by recrystallization from methanol.

2.4.1. 3-(3-(pyridin-4-yl)-4,5-dihydroisoxazol-5-yl)-1H-indole (5j)

Compound **5j** was obtained from 3-(1*H*-indol-3-yl)-1-(pyridin-4-yl)prop-2-en-1-on and hydroxylamine hydrochloride, using the procedure described above.

Light green powder ; mp: 236-238 °C; Yield: 93% ; UV/Vis : λabs (DMSO)/nm : 278; ^{1}H NMR (500 MHz, DMSO-d_6): δ 3.74 (dd, *J=9.5Hz*, *J=17.3Hz*, 1H, CH_2), 3.88 (dd, *J=11.3Hz*, *J=17.3Hz*, 1H, CH_2), 6.21 (dd, J=9.9Hz, *J=11.1Hz*, 1H, CH), 7.00 (m, 1H, Indol), 7.13 (m, 1H, Indol), 7.42(m, 1H, indol), 7.44 (m, 1H, Indol), 7.56 (d, *J= 2.5 Hz*, 1H, Indol), 8.20 (m, 2H, ArH-py), 8.95 (m, 2H, ArH-py), 11.33 (s, 1H, NH); ^{13}C NMR (125 MHz, DMSO-d_6): δ 37.77, 79.83, 111.99, 112.61, 118.67, 119.22, 121.66, 123.12, 124.85, 125.21, 136.85, 143.78, 154.96; HRMS (ESI+) m/z calcd for $C_{16}H_{13}N_3O$ $[M+H]^+$ 264.1137 found 264.1136.

2.5. Biological screening

Biological activities of the prepared compounds were evaluated in view of existing activities for analogous structures. Indeed, chalcones are potential antibacterial and antifungal agents according to the literature [11, 12, 17], whereas oximes are rather known to display antifungal effet [20-b]. For this reason we checked chalcones against bacterial and fungal strains and oximes only against fungi.

2.5.1. In vitro antimicrobial activity

Antimicrobial activity was investigated at the microbiology department of the University Hospital of Tizi-Ouzou, Algeria.

Compounds were tested *in vitro* against microorganisms by the disc diffusion method [31] using Gram-positive bacteria such as *S. aureus* (ATCC 25923), Gram-negative bacteria such as *E. coli* (ATCC 25923) and *P. aeruginosa* (ATCC 27853), and the fungal species *A. niger*, *C. albicans* (ATCC 7102). Mueller Hinton agar and Sabouraud dextrose agar

media were used for antibacterial and antifungal activity respectively.

The concentration of 5.12 mg/mL of the tested compounds was prepared in DMSO and 20 µL of each sample was taken and soaked in 6.0 mm diameter paper discs, the discs were placed on previously seeded plates. The inoculated Petri dishes were prepared using the spore suspension of 10^6 cfu/mL (colony forming unit /mL) previously prepared in sterile physiological water at 0.9 %, with an optical density of 0.08 read at 625 nm. Plates were inoculated with filamentous fungi *A. niger* and incubated at 25°C for six days; *C. albicans* was incubated at 37°C for 24-48 h and Gram positive *S. aureus* and Gram negative *E. coli*, *P. aeruginosa* were incubated at 35-37°C for 24-48 h.

The clear area around each disc was measured in mm. Standard Rifampicin, Cotrimoxazole, Colistin (antibacterial agent) and Fluconazole (antifungal agent) discs were used as positive controls for antimicrobial testing. All experiments were performed in triplicate and the data represent the mean value.

Minimum inhibitory concentrations (MICs) were measured for compounds that exhibited significant zones of inhibition, using the double serial dilution technique. The synthesized compounds were prepared in a concentration range of 500, 250, 125, 62.5, 31.25, 15.62, 7.81 and 3.91 µg/mL. Microdilution susceptibility test was performed in Sabouraud dextrose agar for antifungal activity. MIC is defined as the lowest concentration that showed no microbial growth.

2.5.2. Antioxidant activity studies

The methods and instruments used to measure the activity of antioxidants have made remarkable progress in the past few decades. Early methods measured the efficiency of the antioxidants against the formation of particular species of oxidation products. Thus far, various chemical tests coupled with highly sensitive and automated detection technologies have been used to evaluate antioxidant activity, such as scavenging activity against different types of free radicals (DPPH•), reducing power and metal chelation, among others.

A number of tests are available for the direct measurement of the transfer of the hydrogen atom or the transfer of electrons from antioxidants to free radicals. The antioxidant activities reported in this method group are generally associated with their capacity to neutralize certain types of radical species, out of which some may be artificial and biologically irrelevant. The data regarding the hydrogen atom transfer or the data regarding the donating capacity of the electrons obtained by these methods provide important information on their intrinsic antioxidant potential with minimal environment interference. The method used must have a defined endpoint and chemical mechanism [32].

The DPPH test is a simple technique and requires only a Vis spectrophotometer or an electronic paramagnetic resonance (EPR) spectrometer. However, DPPH• is not a natural radical but the mechanism of reaction with antioxidants is similar to that with peroxyl radicals ROO• [32].

The neutralization DPPH test is based on donating electrons from the antioxidants in order to neutralize the DPPH radical. The reaction is accompanied by changing the DPPH colour measured at 517 nm, and discoloration acts as an indicator of antioxidant activity. Antioxidant activity by the DPPH neutralization method is often reported as EC50, which is defined as the efficient concentration of the antioxidant necessary to reduce the initial DPPH concentration by 50%. In addition, TEC50 may be used, which is the necessary time to reach the equilibrium state with EC50 [33, 34].

The DPPH radical scavenging capacity was measured from the bleaching of purple coloured ethanol solution of DPPH• according to the method described by L.L. Mensor *et al.*, J.S. Lee *et al.* [33, 34]. DPPH• stock solution was prepared by dissolving 4 mg DPPH• in 100 mL ethanol. Compounds **3, 4** and **5j** were dissolved in DMSO to obtain a solution of 10^{-1} M. Test compounds were diluted further with DMSO to get final concentrations of 0.05, 0.025 and 0.0125 mol/l for all the compounds, whereas the standard (ascorbic acid, AA) was diluted to 0.1, 0.05, 0.025, 0.0125, 0.00625, 0.003125, 0.0015625 mol/L solutions respectively. Wells were loaded with 40 µL of tested sample and then with 2 mL of DPPH• solution, all assays being carried out in triplicate. Negative control wells were loaded with 40 µL of DMSO and 2 mL of DPPH• solution. After vortexing, the mixtures were incubated at room temperature for 1 h in darkness at 25 °C, and then the absorbance of the plate was recorded at 517 nm. A blank containing only ethanol with DMSO was used as the control. Each measurement was performed in triplicate.

2.6. In silico Blood-brain barrier prediction

Oximes are known to be antidotes that are used against nerve agents [35] by penetrating through the Blood-Brain barrier. Thus, we used SwissADME web server [36] to estimate the power of Blood-Brain barrier penetration of our synthesized compounds. In addition, the studied compounds were subjected to drug likeness properties study using Lipinski's rule of five.

2.7. Molecular docking studies

2.7.1. Input data preparation

It has been previously reported that organophosphorus insecticides and nerve agents inhibit the enzyme acetylcholinesterase by covalently bonding to the catalytic serine residue of the enzyme. The role of oxime-based reactivators, is to restore the organo-phosphate-inhibited enzymatic activity by cleaving the phosphorous conjugate [37]. These compounds act as agonists of acetylcholine esterase. We wished to evaluate the

potential of our own oximes to act as such. The usual way to evaluate the possibility for a given oxime to displace an organophosphorous inhibitor from the active site is an in silico calculation and molecular dynamics simulations. Thus, the crystal structures of Mus musculus acetylcholinesterase inhibited by the insecticide fenamiphos (fep-mAChE) with PDB ID 2WU4 and resolution of 2.40 Å was downloaded from the RCSB protein data bank and was used for molecular docking study. Thus, the protein was prepared by deleting the substrate cofactors, the crystallographic water molecules, and the co-crystallized ligand Ortho-7 (HBP). Only one monomer was selected and the active site of protein was identified by selecting all residues located at 6 Å from the center of the crystal pose. Thus, the residues Trp86, Tyr341, His447, Phe338, Ile294, Asp74, Trp286, Tyr72, Glu285, Phe297 and Tyr124 were treated as catalytic residues during the docking simulations [38]. On the other hand, the 2D structures of the synthesized compounds and experimental ligand HBP were drawn using MarvinSketch software [39] and were used as flexible ligands during the molecular docking simulation.

2.7.2. Docking procedure

All synthesized compounds were docked into the active site of selected fep-mAChE protein by employing the iGEMDOCK program [40]. Thus, the compounds imported as docking library and the scoring function used was GEMDOCK score. In the docking algorithm, the population size taken was 1000 with 100 generations and 50 numbers of solutions. The resulting dock pose of each ligand docked into protein was analyzed for their hydrogen bond interactions with the receptor and were visualized using AutoDoTools software [41] and Accelrys Discovery Studio Visualizer software version 4.1 [42].

2.8. Molecular dynamics studies

In order to evaluate the stability of studied compounds, the docked conformations with low docking energies were submitted to 20 ns of molecular dynamics simulations [43]. Thus, the Nano Molecular Dynamics software NAMD 2.12 [44] with CHARMM 36 force field was used during the MD simulations. Ligands topologies and parameters were generated using the CHARMM General Force Field (CGenFF) web server. All complexes were solvated in a cubic TIP3P water box of edge length 7 Å and then neutralized and set the concentration of NaCl to the physiological value of 0.15 mol/L [45]. The long/shot contribution interactions were modeled using the particle mesh Ewald (PME) method [46] with a 12 Å nonbonded cutoff and a grid spacing of 1 Å. Periodic boundary conditions (PBCs) [47] were used and temperature and pressure were maintained constant using Langevin thermostat (310 K) and Langevin barostat (1 atm), respectively. Then, the three systems underwent 7000 steps of steepest-descent energy minimization to remove atomic overlaps or improper geometries. After this, studied systems were equilibrated for 100 ps under the constant number of particles, pressure and temperature (NPT). Finally, the obtained systems were submitted to 20 ns of molecular dynamics using 2 fs time steps. Obtained results were visualized and analyzed using VMD software [48].

3. Results and discussion

3.1. Chemistry

In this work, six chalcone oximes **(4a-c, e, h, i)** and one isoxazoline derived from indole **(5j)** were successfully synthesized from the chalcones **(3a-c, e, h, i)** obtained from Claisen-Schmidt condensation by reacting 4-acetylpyridine with different types of aromatic aldehyde substituents under basic conditions [26]. The chalcone **(3j)** was synthesized by piperidine catalyzed Knoevenagel condensation by reacting 4-acetylpyridine with indole-3-carbaldehyde [27]. All the synthesized compounds were characterized by NMR and high and low resolution mass spectrometry. The synthesized compounds were evaluated *in-vitro* for their biological potency against various microorganisms and for their antioxidant potency. The synthesis pathway for these products is described below (**scheme 1).**

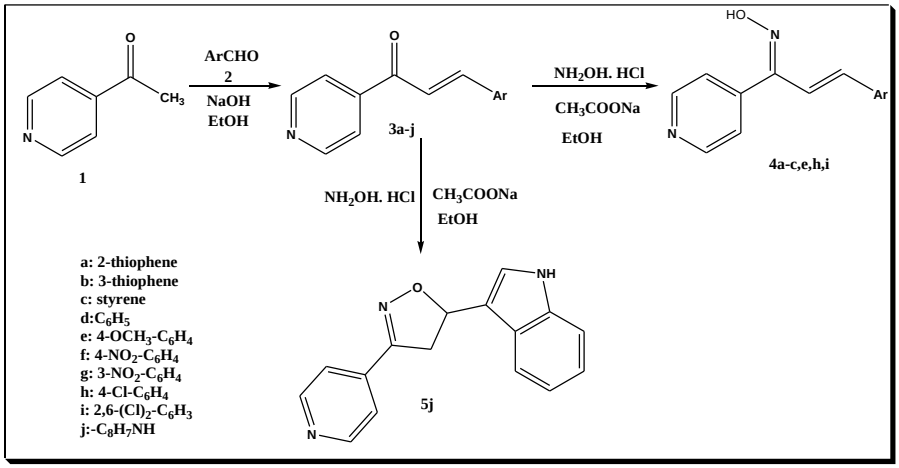

Scheme 1. Synthesis route of oximes chalcones and isoxazoline derived from indole.

In order to optimize the most conceivable and cost-effective reaction conditions, we performed several trials by varying the reaction conditions as reported in the literature for 3-acetylpyridine derivatives [49]. We initiated the synthesis of chalcone by reacting 4-*N*,*N*-dimethylbenzaldehyde with 4-acetylpyridine in an alcoholic medium at room temperature or at reflux [30] for a period of time, in the presence of sodium hydroxide or potassium hydroxide as a base according to the Claisen-Schmidt condensation elaborated in **scheme 1**. After several assays, we concluded that 4-acetylpyridine reacts differently to acetophenone. The chalcone was formed when 4-acetylpyridine was added dropwise to the alcoholic mixture (ethanol or methanol) containing the aldehyde and 10% aqueous NaOH, confirming this work. [26].

Unlike the other chalcones which afforded the expected oximes, chalcone **(3j)** synthesized from indole-3-carboxaldehyde reacted differently in the presence of hydrochlorinated hydroxylamine and sodium acetate. In this case, further cyclization occurred to afford isoxazoline **5j**, the structure of which was well established by 1D (^{1}H, ^{13}C) and 2D NMR, and the chalcone-oxime **(4j)** is a non-isolatable intermediate.

The structures and purities of the resulting products **4** and **5j** were deduced from their NMR data and mass spectrometry. The ^{1}H NMR spectrum of compound **4** shows a singlet around δ_H = 12.60 ppm witch is attributed to the proton resonance of OH of the oxime group. In the case of **5j**, a singlet appeared at δ_H =11.33 ppm, attributed to a proton of isoxazoline ring. The disappearance of the carbonyl peak of chalcone at 189-190 ppm and the supply of a new peak at 152-153 ppm corresponding to C=N of an oxime confirms the formation of this later.

3.2. Spectroscopic study of chalcones (3) and oximes (4), effect of the substituent on the UV-visible spectrum

With the exception of compounds **3i**, **3f** the absorption spectrum of all chalcones shows two bands. a low band ranging from 240 to 244 nm corresponding to the π-π * transition which can only be attributed to the imine group (C = N, aromatic) of pyridine [50] and another very intense band ranging from 260 to 355 nm, attributed to the π-π * transition belonging to the carbonyl group Fig.1 and Table 1. In addition, the absorption spectra of oximes **4** show a single band ranging from 279 to 317 (Fig.2, Table 1) which indicates the disappearance of the carbonyl group and the appearance of a new chromophore, which is the oxime. A hypsochromic effect is observed when passing from the chalcone to the corresponding oxime. Moreover, these results showed that the absorption wavelengths were influenced by the nature and the position of the substituents on the benzene ring.

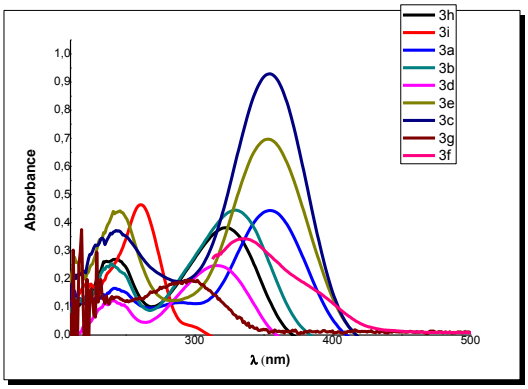

Fig. 1. UV-Visible spectra of chalcones **3** at 3×10^{-5}M ($CHCl_3$).

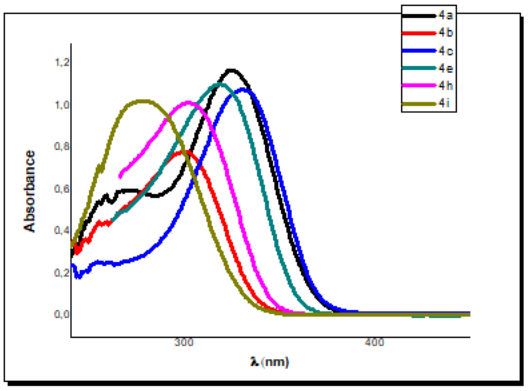

Fig. 2: UV-visible spectrum of the newly synthesized chalcone-oximes **4** at 3×10^{-5} M (DMSO).

The nature of the substituent affects absorption intensities much more than wavelengths. The presence of donor groups by mesomeric effect leads to an increase in absorption intensities (hyperchromic effect) unlike attractant groups.

Table 1. UV-visible spectroscopic characteristics of compounds **3** and **4**.

Compound	λabs (nm)	**Compound**	λabs (nm)

3a	355 π-π* 242 π-π*	**4a**	317 π-π* 270 π-π*
3b	329 π-π* 240 π-π*	**4b**	324 π-π*
3c	354 π-π* 242 π-π*	**4c**	299 π-π*
3d	316 π-π* 242 π-π*	-	-
3e	352 π-π* 242 π-π*	**4e**	329 π-π*
3f	284 π-π*	-	-
3g	296 π-π* 241 π-π*	-	-
3h	320 π-π* 242 π-π*	**4h**	302 π-π*
3i	260 π-π*	**4i**	279 π-π*

3.3. Antimicrobial activity

3.3.1. Antibacterial activity of chalcones (3a-i)

Table 2. Diameters of inhibition zones (mm) of compounds (3a-i) and standard drug at 5.12 mg/mL

Bacterial Strain	**3a**	**3b**	**3c**	**3d**	**3e**	**3f**	**3g**	**3h**	**3i**	**Standard drug***
S.aureus	17 ++	21 +++	15 ++	27 +++	13 +	22 +++	14 +	22 +++	26 +++	20 +++
E. coli	10 +	8 -	6 -	9 +	6 -	6 -	6 -	10 +	9 +	25 +++
P.aeruginosa	10 +	9 +	6 -	9 +	6 -	6 -	6 -	6 -	9 +	30 +++

*Standard drug is Rifampicin for *S.aureus* (5.12 mg/mL), Cotrimoxazole for *E. coli* (5.12 mg/mL), Colistin for *P.aeruginosa* (5.12 mg/mL).

The synthesized heterocyclic chalcones were tested for antibacterial activity against two Gram-negative and one Gram-positive bacteria using the disc diffusion method [31]. Samples were prepared in DMSO at a concentration of 5.12 mg/mL. The muting diameters (mm) are shown in **(Table 2. Fig. 3)**.

In the case of the Gram-positive bacterial strain (*Staphylococcus aureus*, ATCC 25923), it was observed that all synthesized products, had excellent to moderate antibacterial activity. Compound **3d** showed the best inhibition potency, followed by compound **3i**, then compounds **3h**, **3f**, **3b**. Their activity was better than the reference antibiotic (Rifampicin). However, compound **3e** exhibited minimal inhibition. Our compounds proved significantly less active against the other strains: **3a**, **3d**, **3i** showed a slight inhibition against the two Gram-negative bacteria *Escherichia coli* (ATCC 25923) and *Pseudomonas aeruginosa* (ATCC 27853), whereas **3h** exhibited low inhibition only against *E. coli*.

With regard to the structure-activity relationship of the synthesized products, it was noted that **3i**, **3h**, **3f** showed excellent activity against *Staphylococcus aureus* bacteria, indicating that the introduction of strong electron-withdrawing groups (-NO_2, Cl) in the benzene ring increases the antibacterial activity. Conversely, the incorporation of electron donor groups (*p*-OCH_3) on the benzene ring reduces the antibacterial activity (compound **3e**) [51, 52]. Comparing the different substitution positions for chlorine, their order was as follows: 2,6-$(Cl)_2$ > *p*-Cl. This suggests that the introduction of two halogen atoms into the compound may play an important role in increasing the antibacterial properties.

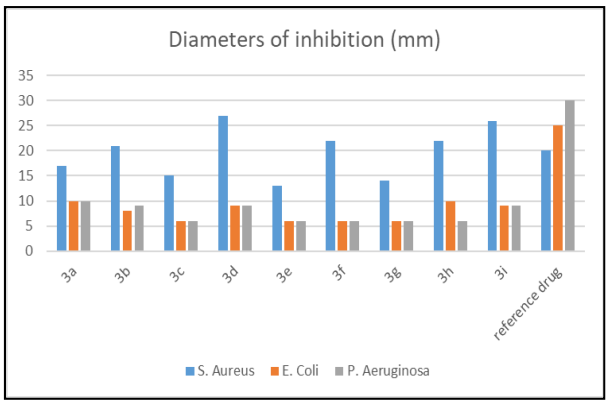

Fig. 3. Inhibition diameters of compounds (3a-i) and of standard drug.

3.3.2. Antifungal activity

The antifungal activity of all synthesized compounds was studied against *A. niger* and *C. albicans*. Inspection of the data **(Table 3, 4)** revealed that compounds **3a**, **3b**, **3d**, **3e** were significantly active against the microscopic fungus *C. albicans*, but still lower than the standard fluconazole taken as reference. Chalcones **3c**, **3f**, **3h**, **3i** were less active, whereas the other chalcones **3g**, **3j** had no effect on the *C. albicans* strain. For *Aspergillus niger*, both compounds **3c**, **3d** showed very good result with maximum inhibition compared to standard drugs followed by compound **3h** which also showed favourable inhibition diameter. The other compounds such as **3a**, **3e**, **3i** showed only slight inhibition. Unlike the results obtained for antibacterial activity, we observed that the presence of the nitro group ($-NO_2$) in the compounds decreases or annihilates the antifungal activity. The variation in the activity of the tested chalcones against microorganisms depends on the impermeability of the cell or differences in the ribosomes of microbial cells. The lipid membrane surrounding the cell favors the passage of any fat-soluble material and it is known that fat solubility is an important factor controlling antimicrobial activity [52].

Table 3. Diameters of inhibition zones (mm) of compounds (3a-j) and standard drug at 5.12 mg/mL

Fungal strain	3a	3b	3c	3d	3e	3f	3g	3h	3i	3j	Standard drug*
A. niger	6	10	19	20	11	6	6	15	11	6	6
	-	+	+++	+++	+	-	-	++	+	-	-
C. albicans	14	14	9	14	14	9	6	11	11	6	29
	++	++	+	++	++	+	-	+	+	-	++++

*Drug: Fluconazole (5.12 mg/mL) for *C. Albicans* and *A. niger*.

Concerning the chalcone-oximes **4**, with the exception of compound **4h** which showed some activity against *C. albicans* (MIC= 500µg/mL) all the other chalcone-oximes **4** and isoxazoline **5j** showed no antifungal activity against the two fungi tested. From these results, it can be concluded that the α,β-unsaturated carbonyl bridge connecting the two rings is important in the mode of action of the compounds against both fungal strains. The results of the antifungal activity are presented in **(Table 3, 4 and Fig.4)**.

The most active products were diluted to evaluate their minimum inhibitory concentrations. Against *C. albicans*, the best result was obtained for the two compounds **3a** and **3b** (MIC= 62.5 µg/mL) followed by compound **3d** (MIC= 125 µg/mL) and finally compound **3e** (MIC= 500 µg/mL). The minimum inhibitory concentrations of the most active compounds remain lower than that of Fluconazole taken as reference (MIC= 15.625 µg/mL).

Against *A. niger*, the best result was obtained with compound **3c** (MIC= 7.8125 µg/mL) followed by compound **3d** (MIC= 15.625 µg/mL) then compound **3h** (MIC= 62.5 µg/mL).

Previous studies [53,54] have shown that the azole-containing drug Fluconazole inhibits the proliferation of the *C. albicans* fungus, but is inactive against *A. niger*. In this work, we were able to demonstrate that six chalcones are active against *A. niger*, three of them showing an excellent result. Based on these data we can assume that the presence of the ketone function or the pyridine ring confers to these molecules an activity against the filamentous fungus *A. niger*.

Table 4. Diameters of inhibition zones (mm) of compounds (4, 5j) and standard drug at 5.12 mg/mL

Fungal strain	4a	4b	4c	4e	4h	4i	5j	Standard drug*
A. niger	6	6	6	6	6	6	6	6
	-	-	-	-	-	-	-	-
C. albicans	6	6	6	6	13	6	6	29
	-	-	-	-	+	-	-	++++

*drug= Fluconazole (5.12 mg/mL) for *C. Albicans* and *A. Niger*.

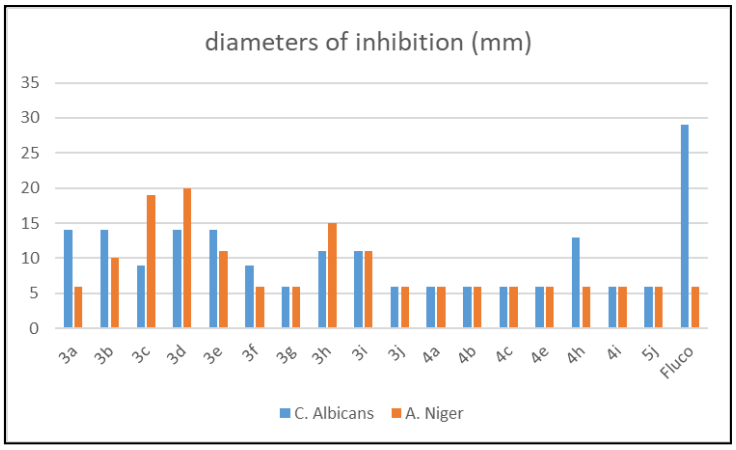

Fig. 4. Inhibition diameters of the synthesized compound and the reference (antifungal agent)

3.4. Antioxidant activity

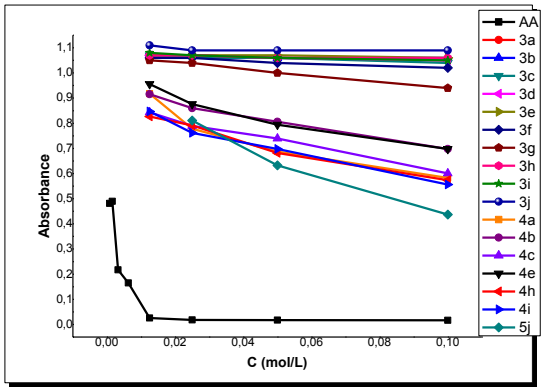

Fig. 5. The variation of absorbance versus concentration of the different compounds 3, 4, 5 and AA.

Antioxidants react with DPPH•, a stable free radical which is reduced to DPPH-H and as a consequence the absorbance is decreased from the DPPH• radical to the DPPH-H form. The degree of discolouration indicates the scavenging potential of the antioxidant compounds in terms of hydrogen-donating ability. All the synthesized compounds **3, 4, 5j** were evaluated for their *in vitro* antioxidant activity by DPPH [33, 34] radical scavenging assay at different concentrations. **Fig. 5** shows the variation of absorbance versus concentration of the different compounds **3**, **4**, **5j** and of the standard ascorbic acid. Lower absorbance of the reaction mixture indicates higher free radical scavenging activity. The capability to scavenge the DPPH• (or inhibition %) was calculated as follows:

RSA (%) = [(Ac - As)/Ac] x 100.

Where Ac is the absorbance of the control (absorbance of DPPH• ethanol solution without sample), and As is the absorbance of the tested compound after 60 min incubation.

It is clear that all the synthesized chalcones **(3a-j)** showed no antioxidant activity, unlike oximes **(4a-c, 4e, 4h, 4i)** and isoxazoline **5j**, which showed moderate activity compared to ascorbic acid taken as reference. The absence of electron-donating substituents on the benzene ring of chalcones, the presence of electron-withdrawing halogen groups or thiophenyl rings explains the absence of antioxidant activity in these molecules.

According to the results obtained, compound **5j** showed the highest activity **(IC_{50}= 16.31 mg/mL)** followed by compound **4h** then **4i**. Compound **4e** showed the lowest antioxidant activity. From these results we could note that in the case of the compound **5j** the cyclization allows the hydrogen of the amine function (NH) present on the indole to be released, which confers it a medium activity contrarily to its precursor **3j**. It was also observed that the position of the heteroatom (sulfur) in the thiophene ring influences the antioxidant activity. The best result was obtained when the sulfur occupies position **2** in the heterocycle. The antioxidant activity of compound **4h** is better than that of compound **4i**, which shows that the presence of chlorine on two positions **(2** and **6)** reduces the antioxidant activity.

3.5. In silico Blood-brain barrier prediction

Blood brain barrier (BBB) penetration is a parameter used to determine whether a compound will penetrate and distribute within the central nervous system (CNS) or if it will be excluded from the CNS. Crossing the BBB is essential for imaging the brain parenchymal and treating for neurological diseases. However, the potency of synthesized oximes to cross the BBB was predicted based on their physicochemical properties and reported in **(Table 5)**. The results show that all synthesized compounds were found to be able to penetrate the blood brain barrier. In addition, none of the synthesized compounds violated the Lipinski's rule of five which is considered as a

prominent principle used in certifying the drug likeness of a compound.

Table 5. BBB penetration and Lipinski rule profile of the studied compounds.

Compound	BBB	Lipinski rule
A (4e)	Penetrate	No violation
B (4h)	Penetrate	No violation
C (4i)	Penetrate	No violation
D (4a)	Penetrate	No violation
E (4b)	Penetrate	No violation
F (4c)	Penetrate	No violation
G (5j)	Penetrate	No violation

3.6. Docking parameters generation

The co-crystallized ligand HBP was extracted from the crystallographic complex **2WU4** and docked in the binding site of fep-mAChE protein **(Fig. 6)**.

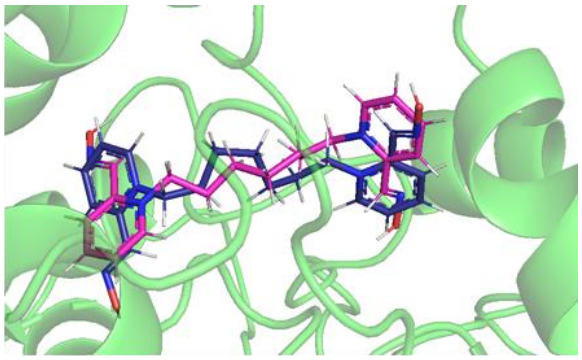

Fig. 6. Superposition of docked conformation (blue sticks) on the crystallographic structure of ligand HBP (magenta sticks). The protein backbone was shown as a green cartoon

The parameters conducting to the acceptable conformation of the ligand in the active site of the protein, characterized by low RMSD from the experimental one, low docking energy [45] and a high number of hydrogen bonds, were used in the docking of synthesized compounds.

3.7. Binding mode of studied compounds

Visualization of the docked conformations of synthesized compounds revealed that all of the studied compounds adopt the same binding mode in the binding site of **2WU4** protein [55], as shown in **(Fig. 7)**.

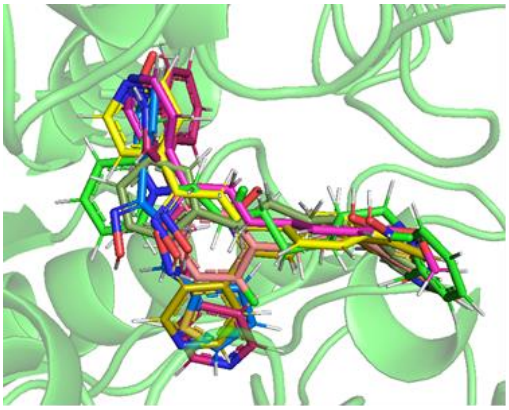

Fig. 7. Superposition of docked conformations of synthesized compounds on the crystallographic ligand (Green sticks)

As shown in **(Fig. 8)** and reported in **(Table 6)**, the compound **G** (**5j**) was involved in hydrogen bonds and hydrophobic interactions with the residues of protein active site of fep-mAChE protein. The nitrogen atom of indole moiety was hydrogen-bonded with the hydroxyl acid of side chain of **Asp74** (3.1 Å), located in the anionic site. Nitrogen atom of the oxazole ring was involved in two hydrogen bonds with the protein, one with carbonyl oxygen of protein backbone of **Trp86** (2.8 Å), located in the choline-binding site, and the second with hydroxyl of **Ser125** (2.9 Å). In addition, the oxygen atom of oxazole moiety was hydrogen bonded with carbonyl amide of **Gln71** (2.8 Å).

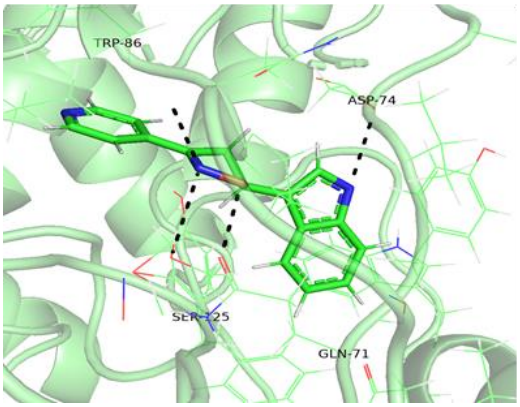

Fig. 8. View of the docked conformation of compound **5j** with fep-mAChE protein.

Besides, compound **G** made attractive and non-covalent π-alkyl and π–π stacked interactions between the carbon atom of oxazole moiety and phenyl ring of indole moiety of this compound and phenyl rings of **Tyr124** and **Tyr72**, respectively. The phenyl ring of **Trp86** is located at 3.78 Å from the pyridine ring of compound **G**, leading to favorable hydrophobic interactions. Also, this compound is surrounded by residues **Phe297**, **Trp286**, **Pro88** and **Leu130** leading to favorable hydrophobic interactions, which may stabilize the ligand in the active site and increase its affinity. It is worth noting that the residues located in the peripheral anionic site at the entrance of the gorge, namely **Tyr72**, **Asp74**, **Tyr124**, **Trp286** and **Tyr341**, constitute a binding site for various reactivators [37].

Table 6. Hydrogen bonds interactions, interacting residues, and docking energies (kJ.mol^{-1}), calculated for synthesized compounds with fep-mAChE protein.

Compound	H-Bond	Interacting residues (< 4 Å)	Docking Energy
A (4e)	His447 (2.8 Å) Asp74 (3.0 Å) Tyr341 (3.1 Å)	π -alkyl : Ile294 π - π stacked : Tyr337 Van der Waals: Tyr72, Trp286, Tyr124, His447, Phe338, Tyr341, Leu76	-104.78
B (4h)	His447 (2.9 Å) Asp74 (3.1 Å) Tyr341 (3.1 Å)	π -alkyl : Tyr72 π - π stacked, π - π T-shaped : Trp286, Tyr337 Van der Waals: Tyr124, Phe338, Leu76	-102.72
C (4i)	His447 (3.1 Å) Thr83 (2.7 Å) Tyr337 (2.6 Å)	π -Sigma: Asp74 Halogen : Trp86 Van der Waals: Trp439, Tyr341, Gly121, Gly82, Leu130, Asn87, Gly126, Gln71, Ser125, Pro88, Tyr72, Val73, Tyr124, Ile294, Phe338	-100.72
D (4a)	His447 (3.1 Å) Tyr341 (2.6 Å)	π -alkyl : Ile294 π - π stacked : Tyr337 Van der Waals: Tyr124, Gly121, Gln71, Ser125, Gly126, Leu130, Gly120, Ala127, Tyr133, Asp74, Phe338	-96.08
E (4b)	Tyr124 (2.0 Å, 3.1 Å)	π - π stacked : Trp286 Van der Waals: Gln71, Val73, Asp74, Pro88, Ser125, Asn87, Thr83, Trp86, Tyr341, Ile294	-94.48
F (4c)	Asp74 (3.0 Å) Tyr341 (2.8 Å) His447 (2.6 Å)	π - π stacked, π - π T-shaped : Tyr72, Tyr124, Tyr337 Van der Waals: Trp286, Ile294, Thr83, Trp86, Phe338, Glu202, Leu76, Gly448	-106.57
G (5j)	Asp74 (3.1 Å) Gln71 (2.8 Å) Ser125 (2.9 Å) Trp86 (2.8 Å)	π - π stacked : Tyr72 π -Alkyl: Tyr124 Van der Waals: Glu285, Trp286, Phe297, Asn87, Pro88, Gly121, Gly126, Leu130, Tyr133	-112.26

Visualization of docked conformations of compounds **A** and **B** shows that only the hydrogen bond with residue **Asp74** was preserved by both compounds **(Fig. 9)**. In addition, the two compounds make hydrogen bonds with nitrogen of imidazole side chain of His447 and hydroxyl group (OH) side chain of **Tyr341** (2.8 Å and 2.9 Å, respectively). Compound **C** with two chlorine groups on the ortho positions of the phenyl ring keeps only the hydrogen bond with nitrogen atom of imidazole moiety of residue **His447** (3.1 Å). Indeed, this compound is involved in two hydrogen bonds with hydroxyl side chain of residues **Thr83** and **Tyr337** (2.7 Å and 2.6 Å).

The replacement of phenyl ring by a heterocyclic thiophenyl ring as in compounds **D** and **E**, leads to a decrease in the docking energies. This is due to the loss of the hydrogen bond interaction with residue **Asp74** (as in compound **D**) and **His447** and **Tyr341** (compound **E**). On the other hand, compound **F** preserves all the hydrogen bonds and the non-covalent π–π stacked interaction observed between compound **A** and the studied protein.

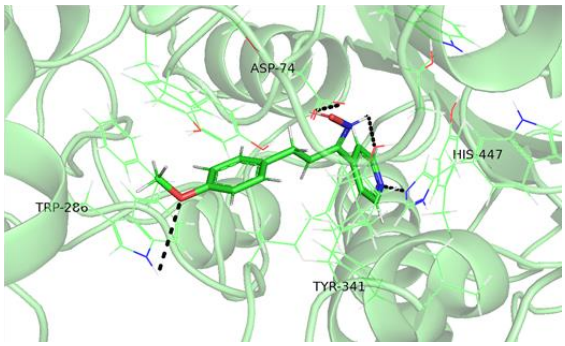

Fig. 9. View of the docked conformation of compound **A** with fep-mAChE protein.

Also, the aromatic rings of residues **Ile294**, **Tyr72**, **Tyr124**, **Tyr337** and **Trp286** are involved in attractive and non-covalent, π-alkyl, π–π stacking, π–π T-shaped with compounds **A**, **B**, **F** and **G**. Besides, the above mentioned attractive and non-covalent interactions were converted to van der Waals interaction in the docked conformation of compound **C**. In addition, this compound was involved in π-sigma and halogen interaction with residues **asp74** and **Trp86**, which may enhance the binding of the compound in the protein active site. On the other hand, compounds **D** and **E** lose all the non-covalent and attractive interactions observed in the docked conformations of other compounds and are simply involved in Van der Waals interactions.

Thereby, docking results revealed that synthesized compounds, were involved in large number of favorable interactions with residues of the active site of fep-mAChE protein. However, to confirm the stability of synthesized compounds in the active site of fep-mAChE protein, we submitted all the docked conformations with low docking energies to molecular dynamics simulation (see below).

3.8. Molecular dynamics simulations

To confirm the binding mode and the stability of docked ligands **A**, **F** and **G** with fep-mAChE protein, molecular dynamics simulations were conducted. The stability of studied systems was evaluated based on change in RMSD of ligands in the protein active site, RMSD of carbons α of protein backbone and Van der Waals interaction energies between compounds and selected protein.

Calculated RMSD plots of protein backbone Cα atoms of studied systems (compound **A- fep-mAChE**, compound **F-fep-mAChE** and compound **G-fep-mAChE**), through the 20 ns of molecular dynamics are reported in **(Fig. 10)**.

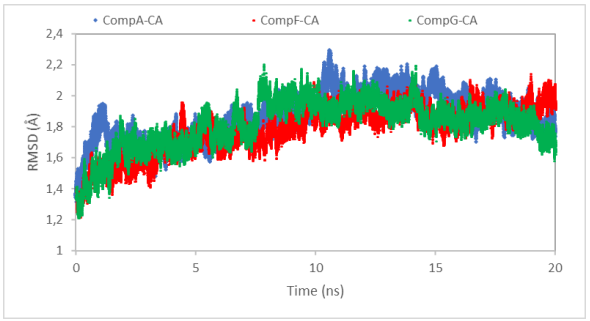

Fig. 10. RMSD plots of backbone Cα atoms of complexes compound **A- fep-mAChE** (blue), compound **F-fep-mAChE** (red) and compound **G-fep-mAChE** (green).

The **(Fig. 10)** shows that the backbone Cα in selected complexes show small fluctuations until 8 ns, where the three systems reach stability at around 1.8 Å of RMSD until the end of simulation. These results indicate that the three complexes are stable through the 20 ns of molecular dynamics simulations.

Calculated RMSD plots of the three studied ligands **A**, **F** and **G**, in the binding site of fep-mAChE protein, through the 20 ns of molecular dynamics are reported in **(Fig. 11)**.

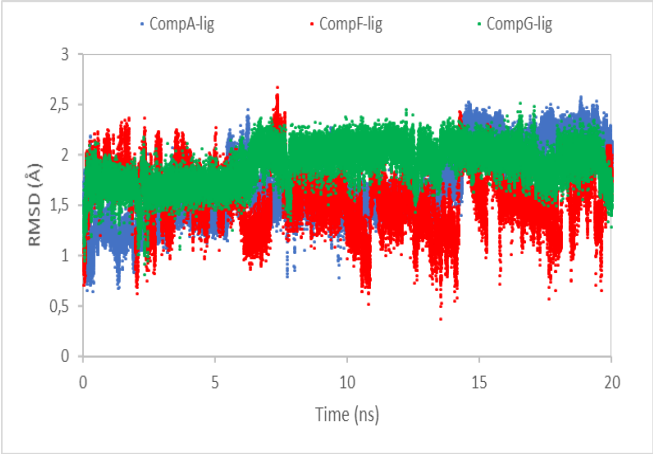

Fig. 11. RMSD plots of the studied compounds **A** (blue), **F** (red) and **G** (green) through the 20 ns of molecular dynamics simulations.

Analysis of results shows some differences between the three curves indicating some movements of studied compounds in the fep-mAChE active site. Thus, RMSD values variation of compounds **A** and **F** ranging from 0.5 Å to 2.3 Å, show ligands flexibility in the active site of fep-mAChE protein [44]. On the other hand, the predicted RMSD curve shape for compound **G** approaches a horizontal line during all the time of simulations, at the average value of RMSD of 1.8 Å, indicating that the compound reaches equilibrium and its change of conformation is very slight.

In order to reveal more mechanistic details, we calculated the interaction energies between the three dynamized compounds and fep-mAChE protein and decomposed them into Van der Waals (VDW) and electrostatic components as shown in **(Fig. 12)**.

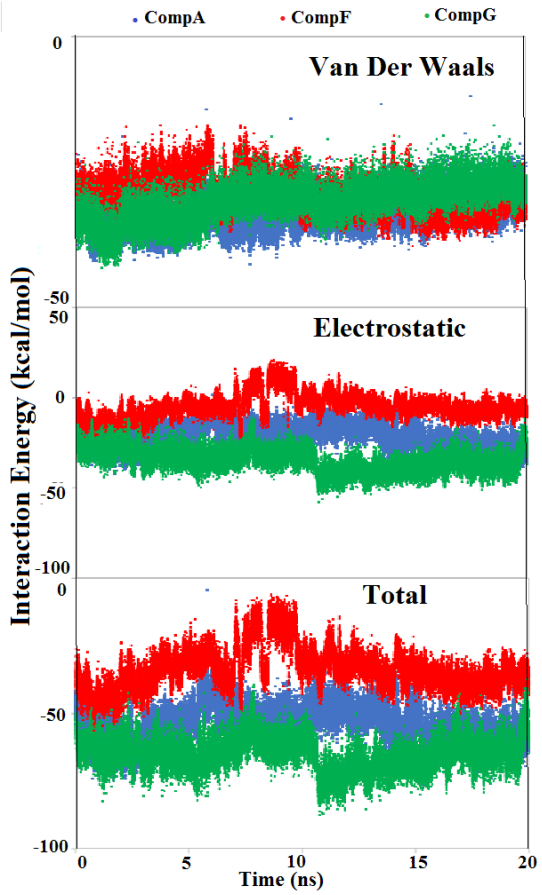

Fig. 12. Plot of Interaction Energy between fep-mAChE and compounds: **A** (blue), **F** (red) and **G** (green) through the 20 ns of molecular dynamics simulation.

The **(Fig. 12)** shows that the calculated VdW energies for three studied compounds are similar with some fluctuations in the first 10 ns with complex compound **F** and fep-mAChE protein. Otherwise, the electrostatic contribution calculated for compound **G** is significant. Therefore, the large electrostatic contribution is mostly due to long-range electrostatic interactions rather than Hydrogen bonding. Indeed, the electrostatic curve shape of this compound approaches a horizontal line at –34 kcal/mol in the first 12 ns of simulation time, where we see a slight decrease. Then, at 16 ns of simulation, the complex compound **G- fep-mAChE** protein resumes the starting conformation until the end of simulation time, where the electrostatic contribution approaches the value of -34 kcal/mol. On the other hand, the VdW interaction energies calculated for compounds **A** and **F** are larger than that of electrostatic one. In addition, the electrostatic interaction energies values calculated for this compound show very little variation under all the simulation time and approaches the value of
-20 kcal/mol. Besides, a few minor fluctuations were observed in the electrostatic contribution curve calculated for compound **F**, between 7 ns and 10 ns of simulation time.

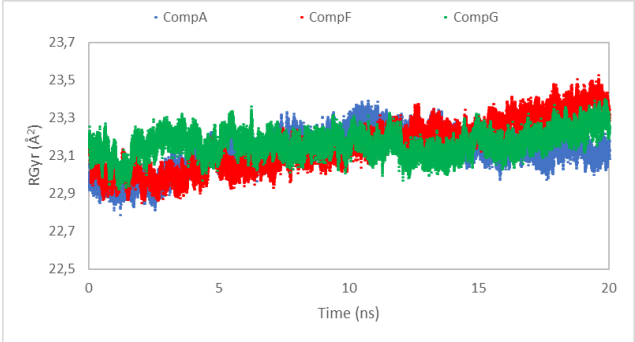

Fig. 13. Radius of gyration plots predicted for the three studied complexes compound **A- fep-mAChE** (blue), compound **F- fep-mAChE** (red) and compound **G-fep-mAChE** (green).

To judge the secondary structure of the fep-mAChE, we track the time evolution of radius of gyration (rGyr) during the time of MD simulation **(Fig. 13)**. The calculated values of rGyr for complexes: compound **A-fep-mAChE**, compound **F-fep-mAChE** and compound **G-fep-mAChE** exhibit lesser fluctuations intensities, revealing that the systems composed of our synthesized compounds **A**, **F**, **G** and fep-mAChE protein arranged to a more compact conformation.

Thereby, molecular docking and molecular dynamics results revealed that synthesized compounds, **A**, **F** and **G**, were involved in large number of favorable interactions with residues of the active site of fep-mAChE protein, which may stabilize the ligands in the active site and increase their affinities.

4. Conclusion

In this work, we have demonstrated that contrary to the oximes, the majority of the 4-acetylpyridine chalcones synthesized have a good antimicrobial activity towards the tested strains. The synthesized oximes presented a better antioxidant activity than the corresponding chalcones although it remains very weak compared to ascorbic acid taken as reference. We observed that the cyclization of the oxime leads to the improvement of the antioxidant activity (compound **5j**). The results of the molecular docking showed that the synthesized compounds could act in a very interesting way as reactivators of the acetylcholinesterase of Mus musculus inhibited by the insecticide fenamiphos (fep-mAChE).

Conflicts of interest

There are no conflicts to declare.

Acknowledgements

The authors would like to thank Dr. Amar Abdoun and Dr. Nadia hadhoum for their help in performing the microbiological tests.

References

[1] K. Bush, P. Courvalin, G. Dantas, J. Davies, B. Eisenstein, P. Huovinen, G.A. Jacoby, R. Kishony, B.N. Kreiswirth, E. Kutter, S.A. Lerner, S. Levy, K. Lewis, O. Lomovskaya, J.H. Miller, S. Mobashery, L.J. Piddock, S. Projan, C.M. Thomas, A. Tomasz, P.M. Tulkens, T.R. Walsh, J.D. Watson, J. Witkowski, W. Witte, G. Wright, P. Yeh, H.I. Zgurskaya, Tackling antibiotic resistance, *Nat. Rev. Microbiol*., 9 (2011) 894–896. https://doi.org/10.1038/nrmicro2693.

[2] S.B. Levy, B. Marshall, Antibacterial resistance worldwide: causes, challenges and responses, *Nat. Med*., 10 (2004) S122–S129.

https://doi.org/10.1038/nm1145.

[3] C. Ghosh, J. Haldar, Membrane-active small molecules: designs inspired by antimicrobial peptides, *Chem. Med. Chem*., 10 (2015) 1606–1624. https://doi: 10.1002/cmdc.201500299.

[4] S.M. Lim, S.A.R. Webb, Nosocomial bacterial infections in intensive care units. I: organisms and mechanisms of antibiotic resistance, *Anaesthesia*, 60 (2005) 887–902.

https://doi.org/10.1111/j.1365-2044.2005.04220.x.

[5] H. Grundmann, M. Aires-de-Sousa, J. Boyce, E. Tiemersma, Emergence and resurgence of meticillin-resistant *Staphylococcus aureus* as a public-health threat, *Lancet*., 368 (2006) 874–885. https://doi.org/10.1016/S0140-6736(06)68853-3.

[6] H.W. Boucher, G.H. Talbot, J.S. Bradley, J.E. Edwards, D. Gilbert, L.B. Rice, J. Bartlett, Bad bugs, no drugs: no ESKAPE! An update from the Infectious Diseases Society of America, *Clin. Infec. Dis*., 48 (2009) 1–12. https://doi.org/10.1086/595011.

[7] T.B. Emran, M.A. Rahman, M.M.N. Uddin, R. Dash, M.F. Hossen, M. Mohiuddin, M.R. Alam, Molecular docking and inhibition studies on the interactions of Bacopa monnieri's potent phytochemicals against pathogenic *Staphylococcus aureus*, *DARU. J. Pharma. Sci*., 23 (2015) 26. https://doi.org/10.1186/s40199-015-0106-9.

[8] M. Xu, P. Wu, F. Shen, J. Ji, K.P. Rakesh, Chalcone derivatives and their antibacterial activities: Current development, *Bioorg. Chem.*, 91 (2019) 103133. https://doi.org/10.1016/j.bioorg.2019.103133.

[9] Y. Zhang, J. Wu, S. Ying, G. Chen, B. Wu, T. Xu, Z. Liu, X. Liu, L. Huang, X. Shan, Y. Dai, G. Liang, Discovery of new MD2 inhibitor from chalcone derivatives with anti-inflammatory effects in LPS-induced acute lung injury, *sci. Rep*., 6 (2016) 25130. https://doi.org/10.1038/srep25130.

[10] Y.H. Chen, W.H. Wang, Y.H. Wang, Z.Y. Lin, C.C. Wen, C.Y. Chern, Evaluation of the anti-inflammatory effect of chalcone and chalcone analogues in zebrafish model, *Molecules*., 18 (2013) 2052-2060.
https://doi.org/10.3390/molecules18022052.

[11] S.A. Lahsasni, F.H.A. Korbi, N.A. Aljaber, Synthesis, characterization and evaluation of antioxidant activities of some novel chalcones analogues, *Chem. Cent. J*., 8 32 (2014). https://doi.org/10.1186/1752-153X-8-32.

[12] H. Iqbal, V. Prabhakar, A. Sangith, B. Chandrika, R. Balasubramanian, Synthesis, anti-inflammatory and antioxidant activity of ring-A-monosubstituted chalcone derivatives, *Med. Chem. Res*., 23 (2014) 4383-4394. https://doi.org/10.1007/s00044-014-1007-z.

[13] U. Sankappa Rai, A.M. Isloor, P. Shetty, K.S.R. Pai, H.K. Fun, Synthesis and in vitro biological evaluation of new pyrazole chalcones and heterocyclic diamides as potential anticancer agents, *Arab. J. Chem*., 8 (2015) 317-321. https://doi.org/10.1016/j.arabjc.2014.01.018.

[14] D.K. Mahapatra, S.K. Bharti, V. Asati, Anticancer Chalcones: structural and

molecular target perspectives, *Eur. J. Med. Chem*., 98 (2015) 69-114. https://doi.org/10.1016/j.ejmech.2015.05.004.

[15] D. Coskun, G.S. Tekin, S. Sandal, M. Faith, G. Coskum, Synthesis characterization

and anticancer activity of new benzofuran substituted chalcones, *J. Chem*., (2016). https://doi.org/10.1155/2016/7678486.

[16] C. Hsieh, T. Hsieh, M. El-shazly, D. Chuang, Y. Tsai, C. Yen, S. Wu, Y. Wu, F. Chang, Synthesis of chalcone derivatives as potential anti-diabetic agents,

Bioorg. Med. Chem. Lett., 22 (2012) 3912-3915. https://doi.org/10.1016/j.bmcl.2012.04.108.

[17] X. Fang, B. Yang, Z. Cheng, D. Zhang, M. Yang, Synthesis and antimicrobial activity of novel chalcone derivatives, *Res. Chem. Intermed*., (2014) 1715-1725. https://doi.org/10.1007/s11164-013-1076-5.

[18] H. Suwito, A.N. Kristanti, N.N.T. Puspanigsih, Chalcones: synthesis structure diversity and pharmacological aspects, *J. Chem. Pharmaceut. Res*., 6 5 (2014) 1076-1088.

[19] S.N. Lopez, M.N. Castelli, S.A. Zacchino, J.N. Dominguez, G. Lobo, J. Charris- Charris, J.C.G. Cortes, J.C. Ribas, C. Devia, A.M. Rodriguez, R.D. Enriz, In viro antifungal evaluation and structure-activity relationships of a new series of chalcone derivatives and synthetic analogues, with inhibitory properties against polymers of the fungal cell wall, *Bioorg. Med. Chem.*, 9 (2001) 1999-2013. https://doi.org/10.1016/S0968-0896(01)00116-X.

[20] (a): B. Baviskar, S. Patel, B. Baviskar, S.S. Khadabadi. Design and synthesis of some novel chalcone as potent antimicrobial agent, *Asian J. Res. Chem*., 1 (2008) 67-69.

(b): Q. Zhang, W. Duan, S. Zhao, J. He, F. Lei, Synthesis, Antifungal Activity and 3D-QSAR Study of Novel (*E*)-Longifolene-Derived Tetralone Oxime

Ethers, Chem.. Select. 6 (18) (2021) 4515-4520. https://doi.org/10.1002/slct.202100898

[21] O. Nerya, R. Musa, S. Khatib, S. Tamir, J. Vaya. Chalcones as potent tyrosinase inhibitors : the effect of hydroxyl positions and numbers, *Phytochemistry*., 65 (2004)1389-1395. https://doi.org/10.1016/j.phytochem.2004.04.016.

[22] J. Lia, C. Chen, F. Wu, L. Zhao, Microwave-assisted synthesis and tyrosinase inhibitory activity of chalcone derivatives, *Chem.Biol.Drug. Des*., 82 (2013) 39-47.

https://doi.org/10.1111/cbdd.12126.

[23] L. Ya-Ting, F. Tsorng-Harn, C. Hui-Min, C. Chao-Yuan, W. Yun-Hsin, C. Ching-Yuh, C. Yau-Hung. Toxicity assessments of chalcone and some synthetic chalcone analogues in a zebrafish model, *Molecules*., 19 (2014) 641-650. https://doi.org/10.3390/molecules19010641.

[24] J. M. Oh, T. M. Rangarajan , R. Chaudhary, R. P. Singh, M. Singh, R. P. Singh, A. R. Tondo, N. Gambacorta, O. Nicolotti, B. Mathew, H. Kim, Novel Class of Chalcone Oxime Ethers as Potent Monoamine Oxidase-B and Acetylcholinesterase Inhibitors, *Molecules*, 25 (2020) 2356. https://doi:10.3390/molecules25102356.

[25] A. Benazzouz-Touami, A. Chouh, S. Halit, S. Terrachet-Bouaziz, M. Makhloufi-Chebli, K. Ighil-Ahriz and A.M.S. Silva, New Coumarin-Pyrazole hybrids: Synthesis, Docking studies and Biological evaluation as potential cholinesterase inhibitors, *J. of Molec. Struc.*, 1249 (2022) 131591. https://doi.org/10.1016/j.molstruc.2021.131591

[26] A. Agarwal, K. Srivastava, S. K. Puri, P. M. S. Chauhan, Synthesis of 2,4,6-trisubstituted pyrimidines as antimalarial agents, *Bioorg. Med. Chem*., 13 (2005) 4645–4650. https://doi.org/10.1016/j.bmc.2005.04.061.

[27] M.N. Peerzada , P. Khan, K.Ahmad , Md. I. Hassan, A. Azam. Synthesis, characterization and biological evaluation of tertiary sulfonamide derivatives of pyridyl-indole based heteroaryl chalcone as potential carbonic anhydrase IX inhibitors and anticancer agents, *Eur. J. of Med. Chem*., 155 (2018) 13-23. https://doi.org/10.1016/j.ejmech.2018.05.034.

[28] N. Sunduru, A. Agarwal, S. B. Katiyar, N. N. Goyal, S. Gupta, P. M. S. Chauhan, Synthesis of 2,4,6-trisubstituted pyrimidine and triazine heterocycles as antileishmanial agents, *Bioorg. Med. Chem.*, 14 (2006) 7706–7715. https://doi.org/10.1016/j.bmc.2006.08.009

[29] S. Alam, R. Panda, M. Kachroo, Anti-tubercular, antioxidant an in vitro anti-inflammatory activity of some newly synthesized chalcones, *Ind. J. of. Chem.*, 5B (2014) 440-443.

[30] R. S. Najem, Synthesis of some pyrimidine derivatives from-4- acetyl pyridine, t*ikrit. J.of. Pure. Sci., 23 3 (2018).*

[31] A. W. Bauer, C. E. Roberts, W. M. Kirby. Single disc versus multiple disc and plate dilution techniques for antibiotic sensitivity testing, *Antibiot. Annu*., 7 (1959-1960) 574-580.

[32] I.G. Munteanu, C. Apetrei, Analytical Methods Used in Determining Antioxidant Activity: A Review. *Int. J. Mol. Sci.* 22 (2021) 3380. https://doi.org/10.3390/ ijms22073380

[33] L.L. Mensor, F.S. Menezes, G.G. Leit~ao, A. S. Reis, C. T.dos Santos , S. C. Coube, S. G. Leitão, Screening of Brazilian plant extracts for antioxidant activity by the use of DPPH free radical method, *Phytother. Res.*, 15 (2001) 127-130. https://doi.org/10.1002/ptr.687.

[34] J.S. Lee, H.J. Kim, H. Park, Y.S. Lee, New Diarylheptanoids from the Stems of Carpinus cordata, *J. Nat. Prod.*, 65 (2002) 1367-1370. https://doi.org/10.1021/np020048l.

[35] F. R. de Souza, D. R. Garcia, T. Cuya, A.S. Pimentel, A. da Silva Gonçalves, R. Bicca de Alencastro, T. C. C. França, Molecular Modeling Study of Uncharged Oximes Compared to HI-6 and 2-PAM Inside Human AChE Sarin and VX Conjugates, *ACS. Omega.*, *5* 9 (2020) 4490-4500. https://doi: 10.1021/acsomega.9b03737.

[36] A. Daina, O. Michielin, V. Zoete, SwissADME: A free web tool to evaluate pharmacokinetics, druglikeness and medicinal chemistry friendliness of small molecules, *Sci. Rep.*, 7 (2017) 42717. https://doi.org/10.1038/srep42717.

[37] A. Hornberg, E. Artursson, R. Warme, Y.-P. Pang, F. Ekstrom, Crystal Structures of Oxime-Bound Fenamiphos-Acetylcholinesterases: Reactivation Involving Flipping of the His447 Ring to Form a Reactive Glu334-His447-Oxime Triad, *Biochem. Pharmacol.*, 79 3 (2010) 507-515. https://doi.org/10.1016/j.bcp.2009.08.027.

[38] S. Bouaziz-Terrachet, A. Toumi-Maouche ,B. Maouche , S. Taïri-Kellou, Modeling the binding modes of stilbene analogs to cyclooxygenase-2: a molecular docking study, *J. Mol. Model.*, 16 12 (2010) 1919–1929. https://doi.org/10.1007/s00894-010-0679-7.

[39] Marvin Sketch program, Chemaxon, http://www.chemaxon.com, 2009.

[40] H. Kai-Cheng, C. Yen-Fu, L. Shen-Rong, Y. Jinn-Moon, iGEMDOCK: a graphical environment of enhancing GEMDOCK using pharmacological interactions and post-screening analysis, *BMC. Bioinf.*, 12 (2011) 1–11. https://doi:10.1186/1471-2105-12-S1-S33.

[41] M.F. Sanner, Python: a programming language for software integration and development, *J. Mol. Graphics. Mod.*, 17 (1999) 57–61.

[42] http://www.accelrys.com

[43] K. Ould Lamara, M. Makhloufi-Chebli, A. Benazzouz-Touami, S. Terrachet-Bouaziz, Nejla

Hamdi, A.M.S. Silva, J. B. Behr, Selectivity control in the reaction between 2-hydroxyarylaldehydes and 4-hydroxycoumarin. Antioxidant activities and computational studies of the formed products, *J. of. Mol. Struc.*, 1231 (2021) 129936. https://doi.org/10.1016/j.molstruc.2021.129936.

[44] J. C. Phillips, R. Braun, W. Wang, J. Gumbart, E. Tajkhorshid, E. Villa, C. Chipot, R.D. Skeel, L. Kalé, K. Schulten, Scalable molecular dynamics with NAMD, *J. Comput. Chem.*, 26 16 (2005) 1781–1802. https://doi.org/10.1002/jcc.20289.

[45] S. Hammad, S. Bouaziz-Terrachet, R. Meghnem, D. Meziane, Pharmacophore Development, Drug-Likeness Analysis, Molecular Docking and Molecular Dynamics Simulations for New CK2 Inhibitors Identification, *J.of. Mol. Model.*, 26 160 (2020) 1-17. https://doi : 10.1007/s00894-020-04408-2.

[46] U. Essman , L. Perera, M.L. Berkowitz, T. Darden , H. Lee, L.G. Pedersen, A smooth particle mesh Ewald method, *J. Chem. Phys.*, 103 (1995) 8577–8593. https://doi.org/10.1063/1.470117.

[47] W. L. Jorgensen, J. Chandrasekhar, J.D. Madura, R.W. Impey, M.L. Klein, Comparison of simple potential functions for simulating liquid water, *J. Chem. Phys.*, 79 (1983) 926–935. https://doi.org/10.1063/1.445869.

[48] W. Humphrey, A. Dalke, K. Schulten, VMD: Visual molecular dynamic, *J. Mol. Graph.*, 14 33 (1996) 33-38. https://doi.org/10.1016/0263-7855(96)00018-5.

[49] M.V. Jyothi, Y. Rajendra Prasad, P. Venkatesh, M. Sureshreddy, Synthesis and Antimicrobial Activity of Some Novel Chalcones of 3-Acetyl Pyridine and their Pyrimidine Derivatives, *Chem Sci Trans.*, 1 3 (2012) 716-722.

[50] A. Atilgan, Ş. Yurdakul,Y. Erdogdu, M.T. Güllüoğlu, DFT simulation, quantum chemical electronic structure, spectroscopic and structure-activity investigations of 4-acetylpyridine, *J. Mol. Struct.*, 1161 (2018) 55-65. https://doi.org/10.1016/j.molstruc.2018.01.080.

[51] M. Xu, P. Wu, F. Shen, J. Ji, K.P. Rakesh, Chalcone derivatives and their antibacterial activities: Current development, *Bioorg. Chem., 91 (2019) 103-133.* https://doi.org/10.1016/j.bioorg.2019.103133.

[52] M.K. Vekariya, D.B. Patel, P. A. Pandya, R. H. Vekariya, P.U. Shah, D.P. Rajani, N.K. Shah, Novel *N*-thioamide analogues of Pyrazolylpyrimidine based Piperazine: Design, Synthesis, Characterization, I*n-silico* molecular docking study and Biological evaluation, *J. of Mol. Stru.*, 1175 (2019) 551-565. https://doi.org/10.1016/j.molstruc.2018.08.018.

[53] M. Mallié, J.M. Bastide, A. Blancard, A. Bonnin, S. Bretagne, M. Cambon, J. Chandenier, V. Chauveau, B. Couprie, A. Datry, M. Feuilhade, R. Grillot, C. Guiguen, V. Lavarde, V. Letscher, M. D. Linas, A. Michel, O. Morin, A. Wade, *In vitro* susceptibility testing of Candida and Aspergillus spp. to voriconazole and other antifungal agents using Etest®: results of a French multicentre study, *Int. J. of Antimi. Agen., 25 4 (2005) 321-328.* https://doi:10.1016/j.ijantimicag.2004.11.010.

[54] K.M. Moghaddam, M. Arfan, J. Rafique, S. Rezaee, P. J. Fesharaki, A. R. Gohari, A. R. Shahverdi, The Antifungal Activity of Sarcococca saligna Ethanol Extract and its Combination Effect with Fluconazole against Different Resistant Aspergillus Species, *Appl. Biochem. Biotechnol*., 162 (2010) 127–133. https://doi 10.1007/s12010-009-8737-2.

[55] S. Bouaziz-Terrachet, R. Terrachet, S. Tairi-Kellou, Receptor and ligand-based 3D-QSAR study on a series of nonsteroidal anti-inflammatory drugs, *Med. Chem. Res.*, 22 4 (2013) 1529–1537. https://doi.org/10.1007/s00044-0120174-z.

Graphical Abstract

Synthesis, biological activities of chalcones and novel 4-acetylpyridine oximes, molecular docking of the synthesized products as acetylcholinesterase ligands

Leave this area blank for abstract info.

Kamilia Ould Lamara,[a] Makhloufi-Chebli Malika,[a] Amina Benazzouz-touami,[a] Souhila Terrachet-Bouaziz,[b,c] Anthony Robert,[d] Carine Machado-Rodrigues,[d] Jean-Bernard Behr [d**]*

[a]*Laboratoire LPCM, Département de Chimie, Faculté des Sciences, Université Mouloud Mammeri, 15000, Tizi-Ouzou, Algeria.*

[b] *Department of Chemistry, Faculty of Sciences, University Mohamed Bouguerra, Boumerdes, Algeria.*

[c] *Laboratoire de Physico-Chimie Théorique et de Chimie Informatique, Faculté de Chimie, USTHB, BP 32 El Alia, 16111 Bab-Ezzouar, Alger, Algeria.*

[d]*Université de Reims Champagne –Ardenne, Institut de Chimie Moléculaire de Reims (ICMR), CNRS UMR 7312, UFR Sciences Exactes et Naturelles, BP 1039, 51687 Reims Cedex 2, France.*

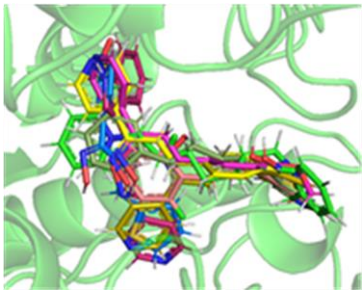

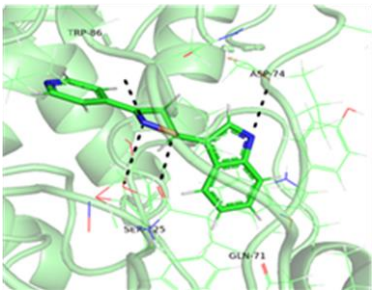

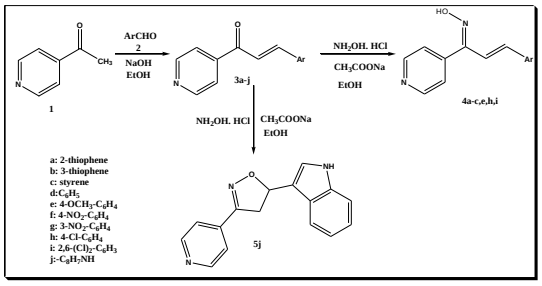

To create your abstract, type over the instructions in the template box below.
Fonts or abstract dimensions should not be changed or altered.